

# Regulation of Cyclin D1 and p16<sup>INK4A</sup> Is Critical for Growth Arrest during Mammary Involution<sup>1</sup>

Michele Gadd,<sup>2</sup> Carmen Pisc,<sup>2</sup> John Branda, Viviana Ionescu-Tiba, Zeljko Nikolic, Chuanwei Yang, Timothy Wang, Gregory M. Shackleford, Robert D. Cardiff, and Emmett V. Schmidt<sup>3</sup>

Massachusetts General Hospital Cancer Center, Charlestown, Massachusetts 02129 [M. G., C. P., J. B., V. I.-T., Z. N., C. Y., G. M. S., E. V. S.]; Department of Surgical Oncology, Massachusetts General Hospital, Boston, Massachusetts 02114 [M. G.]; Department of Medicine, University of Massachusetts Medical School, University of Massachusetts Memorial Healthcare, Worcester, Massachusetts 01655 [T. W.]; Department of Pathology, School of Medicine, University of California at Davis, Davis, California 95616 [R. D. C.]; The Pediatric Service, Massachusetts General Hospital, Boston, Massachusetts 02114 [Z. N., E. V. S.]; and Division of Hematology-Oncology, Children's Hospital of Los Angeles, Los Angeles, California 90027 [G. M. S.]

## ABSTRACT

A coordinated growth arrest during mammary involution completes the dramatic changes in mammary cell proliferation seen during pregnancy and lactation. Signals regulating this arrest are poorly understood, despite their potential relevance to oncogenesis. Here we report that the arrest involves a unique pulse of p16<sup>INK4A</sup> expression *in vivo*, which accompanies decreased cyclin D1 expression and a shift to an active repressor E2F4 complex. We used INK4A/ARF<sup>-/-</sup> mice as well as cyclin D1 and p16<sup>INK4A</sup> transgenic strains to examine the physiological significance of these patterns. p16<sup>INK4A</sup> directly regulated the *in vivo* transition from E2F3 to E2F4 as the major E2F DNA binding activity, and its contribution to growth arrest was independent of cyclin D1. Transgenic cyclin D1 expression prevented normal terminal differentiation by ablating the p16<sup>INK4A</sup> pulse, abolishing the shift from E2F3 to E2F4, derepressing E2F target genes, and expanding a stem cell population. The effects of cyclin D1 were reversed by restoring p16<sup>INK4A</sup> but were not seen in INK4A/ARF<sup>-/-</sup> mice. Our results indicate that cyclin D1 may contribute to tumorigenesis by altering cell differentiation and demonstrate a significant function for p16<sup>INK4A</sup> in development *in vivo*. These regulatory mechanisms used during mammary involution offer a potential explanation for the protective effect of pregnancy against breast cancer.

## INTRODUCTION

Significant variations in breast cancer rates in different countries identify nongenetic factors as particularly important contributors to breast cancer (1). These variations are often attributed to simple cultural differences in the timing or numbers of pregnancies, but mechanisms by which these factors might alter breast cell proliferation remain unclear (2, 3). Rodent models identify a terminal differentiation event that alters the subsequent proliferative potential of the mammary gland by decreasing mammary stem cell numbers during involution (4, 5). We sought to identify molecular signals that might mediate this terminal differentiation event.

We focused on the regulation of cyclin D1 and its regulatory pathway because it is uniquely important in mammary development (6, 7). Moreover, cyclin D1 is located in a region on chromosome 11q13 that is commonly amplified and overexpressed in breast cancers (8, 9). The appearance of adenocarcinomas in MMTV<sup>+</sup>-cyclin D1 transgenic mice demonstrates the oncogenic potential of cyclin D1 (10). Compared with other tissues (10–13), its potency in mammary tissues suggests that cyclin D1 may exhibit activities that uniquely contribute to mammary tumorigenesis.

Received 2/21/01; accepted 10/30/01.

The costs of publication of this article were defrayed in part by the payment of page charges. This article must therefore be hereby marked *advertisement* in accordance with 18 U.S.C. Section 1734 solely to indicate this fact.

<sup>1</sup> This work was supported by Grant RO1 CA69069 from the National Cancer Institute of the NIH.

<sup>2</sup> The first two authors contributed equally to this work.

<sup>3</sup> To whom requests for reprints should be addressed, at Massachusetts General Hospital Cancer Center, Building 149, 13th Street, Charlestown, MA 02129.

<sup>4</sup> The abbreviations used are: MMTV, mouse mammary tumor virus; EMSA, electrophoretic mobility shift assay.

Cyclin D1 works in concert with kinase partners (Cdk4/6) to phosphorylate pRb, which then regulates the E2F transcription complex. Release of active free E2F from inactive complexes with pRb may regulate some E2F-dependent transcriptional activation of genes controlling DNA synthesis (14). An alternative view holds that active repressor E2F/pRb complexes are the more significant regulators (15). Several growth-suppressing pathways converge on cyclin D1 and its kinase partners (16). Among the specific inhibitors, INK4A (p16) is especially interesting considering the frequency of p16<sup>INK4A</sup> mutations in human cancers (17) and its frequent inactivation in breast cancers (18, 19).

Although perturbations in cyclin D1/Cdk4, p16<sup>INK4A</sup>, or pRb are central to tumorigenesis (17), overexpressed G1 cyclins generally do not increase net cell proliferation, despite accelerating G<sub>1</sub> to S progression (20). This paradox remains unresolved, especially *in vivo*. In contrast, the contribution of cell cycle regulators to alterations in terminal differentiation pathways has obvious implications for tumorigenesis (21–23). Here we report that regulated changes in cyclin D1 and p16<sup>INK4A</sup> independently contributed to aspects of growth arrest during normal mammary involution.

## MATERIALS AND METHODS

**Plasmids, Cell Lines, and DNA Constructs.** Plasmids used included pGEM-cyclin D1 (24) and pBS-p16 provided by Drs. Jim Koh and Ed Harlow (25). Dr. Charles Sherr provided plasmids containing murine cDNAs for cyclin D1 (26), p16<sup>INK4A</sup> (27), and p19<sup>INK4A</sup>BARF (28). pMMTV-p16 was constructed by replacing CMV enhancer and promoter sequences in pCMV-p16 (25) with the MMTV enhancer and promoter from plasmid pA9 (Ref. 29; Fig. 2). An injection fragment used to make transgenic mice was isolated from plasmid sequences by cutting at *Hind*III and *Nde*I sites. NIH3T3, murine erythroleukemia cells (MEL), and SAOS2 cells were obtained from the American Type Culture Collection.

**Animals and Histology.** FVB inbred mice (Taconic Farms, Germantown, NY) were bred for analysis of gene expression. Unless otherwise noted, pregnancy samples were obtained on day 10 after vaginal plugs were identified. Lactation samples were obtained from mice 10 days after litters were born for most studies. Day two of lactation was used to evaluate the phenotype of MMTV-p16 mice losing litters. Involution was studied by removing pups from their mother on day 10 and obtaining samples on the indicated day after weaning (30). MMTV-cyclin D1 mice were described previously (10). Mammary glands were fixed in 4% paraformaldehyde in PBS for histological preparations. Whole mounts were prepared by dissecting the mammary fat pad from the pelt, fixing in 10% buffered formalin, staining with hematoxylin, dehydrating in graded series of alcohol, and clearing with xylene.

Immunostaining was performed using commercial antibodies (Santa Cruz Biotechnology) to mouse p16, human p16, and human cyclin D1 (HD11). For immunohistochemical staining, nonspecific mouse IgG1 was used as a negative control reagent. The detection reaction used the Vector Elite ABC kit (Vector, Burlingame, CA).

Eight lines of transgenic mice were developed by microinjection of the MMTV-p16 fragment using standard methods (10). For this study, we concentrated on mice of the TG.MI6 and TG.MI2 line, which demonstrated physiological and attenuated levels of INK4A expression. All animals received

humane care following study guidelines established by the Massachusetts General Hospital Subcommittee on laboratory animal care.

**MMTV Infection and Analysis for Proviral Integrants.** Virgin female mice were infected with MMTV by i.p. injection of  $10^7$  EH-2 cells at 5–8 weeks of age. EH-2 is a rat XC cell line that produces a pathogenic hybrid MMTV consisting primarily of MMTV(C3H) sequences (31). To assay for infectious MMTV provirus in tumors, *Bgl*III-digested genomic DNAs were hybridized with a 1.2-kb *Bam*HI *env* probe from the parent plasmid, pUVH. We probed *Hind*III cut tumor DNA with the 1.2-kb *Bam*HI *env* probe to detect 3' flanking sequences and with a 2.4-kb *Xho*I-*Eco*RI *gag-pol* probe to detect 5' flanking sequences. Finally, we probed *Bgl*III cut tumor DNA with a 2.5-kb *Eco*R V *pol* probe that hybridized with endogenous proviral sequences to control for DNA loading.

**Protein and RNA Expression Studies.** Dr. Rob Hurford kindly provided protein lysates from Rb<sup>+/+</sup> and Rb<sup>-/-</sup> cells. Protein samples were obtained from mammary tissues by crushing mammary glands frozen in liquid nitrogen using a mortar and pestle (32). Mammary lysates were made by passing the resulting powders through a 20-gauge needle at 4°C in TNE buffer (50 mM Tris, 420 mM NaCl, 2 mM EDTA, 0.5% NP40, pH 8.0) and centrifugation to remove debris. Protein expression was determined using standard immunoblots containing 50  $\mu$ g of total protein. Membranes were cut according to molecular weights of the proteins to be identified, and individual blots were successively incubated with the indicated following antibodies: (a) from Drs. Jim Koh and Ed Harlow: JC1 mouse monoclonal that specifically recognizes human p16<sup>INK4A</sup>, JC2 and JC8, which specifically recognize both mouse and human p16<sup>INK4A</sup>; (b) from Dr. Chuck Sherr: rabbit polyclonal antibodies against peptides for murine p18<sup>INK4C</sup> and p19<sup>INK4D</sup> (33); and (c) a commercial mouse monoclonal antibody against actin (Boehringer). Secondary antibodies used were those included in an enhanced chemiluminescence detection kit (Amersham).

RNA blots were performed by standard techniques (10). RNase protection assays were performed using a kit from the Promega Corp. following the enclosed instructions.

**EMSAs.** Tissue extracts for EMSAs were prepared from powdered mammary tissues by a modification of the Dignam method using extraction buffer [20 mM HEPES (pH 7.9), 0.42 M NaCl, 1.5 mM MgCl<sub>2</sub>, 0.2 mM EDTA, 0.5 mM phenylmethylsulfonyl fluoride, 0.5 mM DTT, and 25% glycerol]. Binding reactions included 10  $\mu$ g of the indicated extracts. Gel shift activity was evaluated in standard EMSA binding buffer [20 mM HEPES (pH 7.4), 10 mM KCl, 0.1 mM EDTA, 1 mM DTT, 1 mM MgCl<sub>2</sub>, and 5% glycerol] with salmon sperm DNA (0.1  $\mu$ g/ $\mu$ l) as nonspecific competitor. Subsequently, complexes were resolved on 6 or 5% (for supershifts) nondenaturing polyacrylamide gels containing 1 $\times$  TBE [0.09 M Tris-borate (pH 8.0), 0.002 M EDTA].

After labeling with [ $\gamma$ -<sup>32</sup>P]ATP using polynucleotide kinase, double-stranded oligonucleotides were purified by PAGE. The E2F consensus oligonucleotide contained the following sequence in the sense orientation: E2F consensus, ATTTAAGTTTCGCGCCCTTCTCAAATTT. Each binding reaction contained between 0.1 and 0.5 ng of labeled oligonucleotide. Competition experiments were performed using the indicated molar excess of unlabeled oligonucleotides. For supershift analyses, the following antibodies were added to the binding reaction: E2F-1, KH129 (2.0  $\mu$ l); E2F-2, L-20 (2.0  $\mu$ l; Santa Cruz Biotechnology); E2F-3, C-18 (2.0  $\mu$ l; Santa Cruz Biotechnology); E2F-4, WuF10 (2.0  $\mu$ l); E2F-5, 274 (2.0  $\mu$ l); DP1, WTN10 (2.0  $\mu$ l); Rb, C-15 (2.0  $\mu$ l; Santa Cruz Biotechnology); and p107, SD-15 (1.0  $\mu$ l); p130, C-20 (0.5  $\mu$ l; Santa Cruz Biotechnology).

## RESULTS

**Regulation of Cyclin D1 and INK4A (p16) in Mammary Glands Contributes to Regulation of E2F4 Activity during Mammary Involution.** The proliferative cycle of pregnancy includes several stages: (a) branching ductular proliferation during pregnancy; (b) lobuloalveolar proliferation and differentiated function during lactation; (c) growth arrest accompanied by a marked decrease in subsequent proliferative potential in the initial stages of involution (terminal differentiation); and (d) rapid tissue regression culminating in a return to normal cellularity 7 days after weaning (Fig. 1; Ref. 34). To identify patterns of regulation of cell cycle control genes during mammary involution, we compared expression of cyclin D1 and p16

on days 1, 2, 3, 5, and 7 after lactation with expression in mammary glands from virgin mice, pregnant mice on day 10, and lactating mice on day 10. Gene expression did not change throughout other time points in the estrous cycle of virgin mice, throughout pregnancy, or at any other time point during lactation.

Cyclin D1 remained at relatively constant levels in virgin mice and throughout pregnancy (Fig. 1, A and C). Cyclin D1 then decreased significantly to very low levels on days 1, 2, and 3 after weaning and returned to prepregnancy levels on days 5 and 7 of involution. Following a pattern that was nearly the inverse of cyclin D1, p16<sup>INK4A</sup> protein appeared only on days 2, 3, and 5 after weaning and was absent from virgin mice, throughout pregnancy and throughout lactation (Fig. 1, A and D).

Although cyclin D1 is thought to regulate the G<sub>1</sub>-S transition by phosphorylating pRb, it remains unresolved whether free activating E2F or E2F-pocket protein repressor complexes ultimately mediate these effects *in vivo*. We therefore examined the functional status of E2F activity *in vivo* using EMSA coupled with supershift assays for the various E2Fs, DP1, and pocket protein family members. We focused on E2F activities as the critical readouts of the pRb pathway. Both cyclin-dependent kinase activity and pRb concentrations were too low *in vivo* for us to reliably detect changes. By comparing samples from actively growing tissues during lactation to histologically identical samples obtained 2 days later during mammary involution, patterns characteristic of growth arrest could be identified. The predominant E2F activity during lactation was supershifted by anti-E2F3 antibodies in wild-type mice (Fig. 1E, compare Lanes 1, 3, and 4). The predominant E2F activity during involution was supershifted by anti-E2F4 antibodies (Fig. 1E, compare Lanes 5, 7, and 8). In contrast, E2F activity was not supershifted by anti-E2F1, 2, or 5 antibodies in any stage of mammary development in any mice, and all complexes contained DP1 (not shown).

Given the association of the cyclin D1 and p16 regulation with changes in E2F activity that were consistent with the growth-inhibiting functions of E2F4, we sought to determine whether p16 contributes directly to the shift from E2F3 to E2F4 or to formation of pocket protein complexes. To answer this question, we obtained a knockout strain of mice that is nullizygous for the *p16* locus (including both the p16<sup>INK4A</sup> transcript and the p19<sup>BARF</sup> transcript; Ref. 35). We first evaluated E2F activity in these INK4A/ARF<sup>-/-</sup> mice (Fig. 1F). We found no change in E2F EMSA activity during lactation in p16 nullizygous mice, consistent with its normal absence during that stage (not shown). However, E2F complex formation was lost in the INK4A/ARF<sup>-/-</sup> mice during involution (Fig. 1F, Lanes 1 and 3). The predominant binding activity was again E2F4 (Lanes 7 and 8), but the loss of p130-E2F interactions was apparent in supershift experiments (Lanes 9 and 10).

Growth arrest, terminal differentiation, and tissue regression occur together during normal mammary involution (34). To evaluate the role of the physiological pulse of p16<sup>INK4A</sup> in these processes, transgenic p16<sup>INK4A</sup> was targeted to mammary glands. Using MMTV enhancer and promoter sequences to regulate transcription, we targeted expression of a human p16<sup>INK4A</sup> cDNA (25) to mammary epithelium (Fig. 2A). We focused our studies on two transgenic lines among several founder lines that exhibited physiologically significant levels of p16. The higher expressing line was designated Tg.MI6 and expressed p16 at levels similar to those found during normal mammary involution. A strain with lower expression levels was termed Tg.MI2. Transgenic expression appeared in virgin mice immediately after puberty and was seen during all subsequent stages of mammary growth and development as expected of an MMTV-driven transgene.

The MMTV-p16 transgenic mice demonstrated a direct contribution of the pulse of p16 to the developmental switch to E2F4 and to

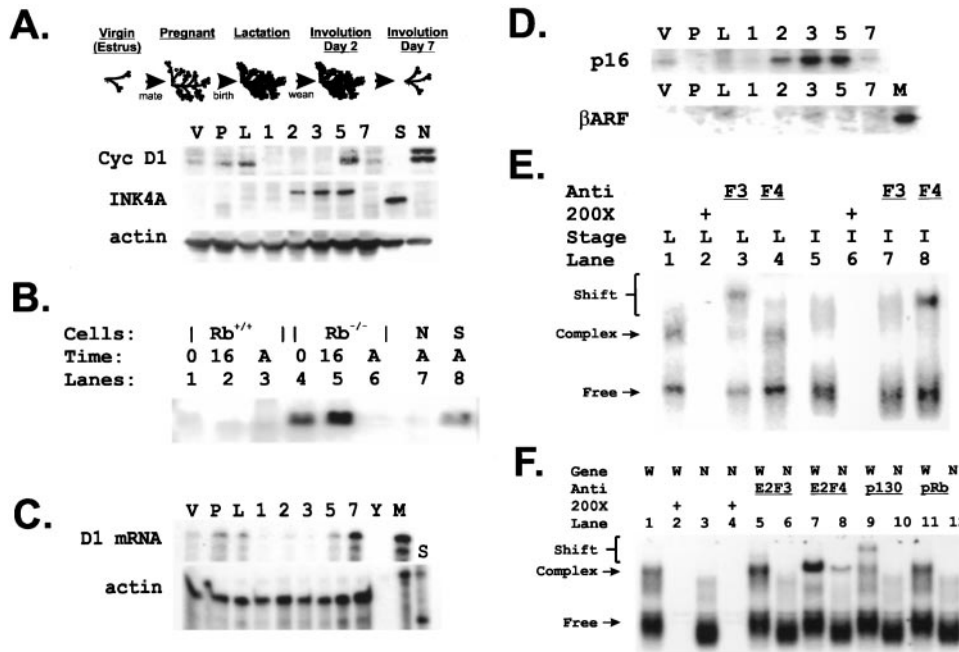


Fig. 1. A pulse of p16<sup>INK4A</sup> accompanies decreased cyclin D1 expression during mammary involution. **A**, cyclin D1 (*Cyc D1*), p16<sup>INK4A</sup> (*INK4A*), and actin were compared in immunoblots containing mammary lysates from virgin (V), pregnant (P), and lactating (L) mice, as well as from mice sacrificed on involution days 1, 2, 3, 5, and 7. Controls included NIH3T3 (N) and SAOS2 (S) cells. **B**, we validated cross-species reactivity of the JC8 monoclonal antibody to p16<sup>INK4A</sup> (*INK4A*) using protein lysates from murine fibroblasts, murine NIH3T3 cells, and human SAOS2 cells. Murine fibroblasts derived from Rb<sup>+/+</sup> and Rb<sup>-/-</sup> embryos were growth arrested in serum-free medium for 0 or 16 h to elicit expression of p16<sup>INK4A</sup> (*Time*) and compared with asynchronously growing cells (*A*). **C**, cyclin D1 mRNA detected in RNase protection assays was present in virgin (V), pregnant (P), and lactating (L) glands but disappeared on involution days 1, 2, and 3. An actin control and size markers (S) are indicated. Additional controls included yeast (Y) tRNA and NIH3T3 cell mRNA (M). **D**, Northern blots containing the same RNAs as in **C** were probed with transcript-specific fragments that detected p16<sup>INK4A</sup> alone (*p16*) or the alternative reading frame ( *$\beta$ ARF*) of the *INK4A* locus. RNA from murine erythroleukemia cells (M) was used as a positive control for the  *$\beta$ ARF* transcript. **E**, EMSAs compared E2F activities in lactation (L) and involution (I). Cold competitor oligonucleotides were included ( $\times 200$ ; *Lanes 2 and 6*) to evaluate specificity of E2F binding. E2F proteins bound as free E2F (*Free*) or as complexes with pocket proteins of the pRb family (*Complex*). Supershifted E2F activities (*Shift*) were only detected in mammary extracts using antibodies either to E2F3 (*Lane 3*) or E2F4 (*Lane 8*). No supershifts were seen with E2F1, 2, or 5 antibodies. **F**, an EMSA compared E2F activity in INK4A/Arf<sup>-/-</sup> (*Gene N*) mammary glands with wild-type glands during involution (*Gene W*). Specific activity was demonstrated by cold competitions ( $\times 200$ ). A comparison of *Lane 3* to *Lane 1* demonstrated decreased E2F/pocket protein complexes in the p16 nullizygous mice. The activities were predominately E2F4, as indicated by the supershifts in *Lanes 7 and 8* (*Anti F4*). An antibody to p130 (*Anti p130*) supershifted the complexed activity in the wild-type (*Lane 9*) but not the p16 nullizygous mice (*Lane 10*). Supershifts were not seen for pRb (*Anti pRb, Lanes 11 and 12*).

formation of E2F4-pocket protein complexes. We used Tg.MI2 mice for these biochemical studies because the Tg.MI2 mice lost their litters on day 2 of lactation, a time point preceding those used to study the normal mice. Premature expression of p16 induced E2F4 activity in the MMTV-p16 mice during lactation (Fig. 2B). Although addition of anti-E2F3 supershifted the E2F-complex in normal mice (*Lane 1 versus Lane 5*), no E2F3 supershift occurred in the MMTV-p16 mice (*Lane 3 versus Lane 6*). In contrast, addition of anti-E2F4 supershifted the E2F-complex in MI2 mice (*Lane 3 versus Lane 8*), and no E2F4 supershift occurred in the wild-type mice during lactation (*Lane 1 versus Lane 7*). Increased E2F4-pocket protein complex formation supplemented this effect in the MMTV-p16 transgenic mice during involution (Fig. 2C). This was most evident in a comparison of the ratio of complexed-E2F to free E2F in the involuting MMTV-p16 mice (compare *Lanes 3 and 1*). This complexed E2F in the MMTV-p16 mice remained E2F4 (*Lane 3 versus Lane 7*), as seen previously in the wild-type mice (*Lanes 1 and 7* here, and *Lanes 1 and 7* in 1E). The pocket protein involved in the E2F4 complexes changed from the p130 observed in the wild-type mice to pRb (compare *Lanes 1 and 9*). Instead, antibodies to pRb supershifted the complexes in the MMTV-p16 transgenic mice (*Lanes 3 and 12*).

We used immunohistochemical techniques to demonstrate endogenous p16 protein expression in mammary epithelial cells lining lobuloalveolar structures during involution (Fig. 3B).

Increased cellular growth rates, delayed growth arrest, or decreased tissue regression should increase epithelial cellularity at the end of mammary involution in INK4A/ARF<sup>-/-</sup> mice if p16 alone was sufficient to regulate those processes in mammary involution. We

evaluated standard histological sections and found that p16 loss did not alter cellularity in mammary glands of INK4A/ARF<sup>-/-</sup> mice (Fig. 3, C and D). To evaluate the possibility that other INK4 proteins functioned in a redundant manner with p16, we stained histological sections using antibodies to p18<sup>INK4C</sup> and p19<sup>INK4D</sup> (Fig. 3, E and F). Both proteins were expressed in the same cells as p16<sup>INK4A</sup>. Finally, we did not observe expression of either p15<sup>INK4B</sup> (not shown) or p16 locus- $\beta$  alternative reading frame (p19 <sup>$\beta$ ARF</sup>) transcripts (Fig. 1D) in mammary tissue in any developmental stage.

**Premature Expression of p16<sup>INK4A</sup> in Mammary Epithelium Arrests Lobuloalveolar Development during Lactation.** Although redundant expression of p18 and p19 proteins may preclude appearance of a mammary phenotype in the INK4A/ARF<sup>-/-</sup> mice, transgenic p16<sup>INK4A</sup> caused an obvious phenotype in the MI6 strain (Fig. 2, D-F, and Fig. 3, G-M). Sixty % of litters born to MI6 mothers died during their mothers' first pregnancies (Fig. 2, D, MI6 column;  $P < 0.01$  by  $\chi^2$  analysis). The pattern of litter loss was consistent. Mothers initially fed their pups. All pups then died within the first 3 days of lactation, irrespective of the pups' genotypes. Mammary glands of MI6 mothers losing their litters showed a marked loss of the ability to proliferate along lobuloalveolar lineages when compared with wild-type siblings (Fig. 3, compare I with H). Most of the ducts completely lacked alveoli and secretions (see arrows). These changes were apparent in thin ductular branches lacking alveoli and milk, which appeared within a background of ductular structures exhibiting more normal alveolar development. Immunostaining demonstrated the presence of transgenic p16 protein in the epithelial cells lining ductular and lobuloalveolar structures (Fig. 3G). Finally, whole-mount



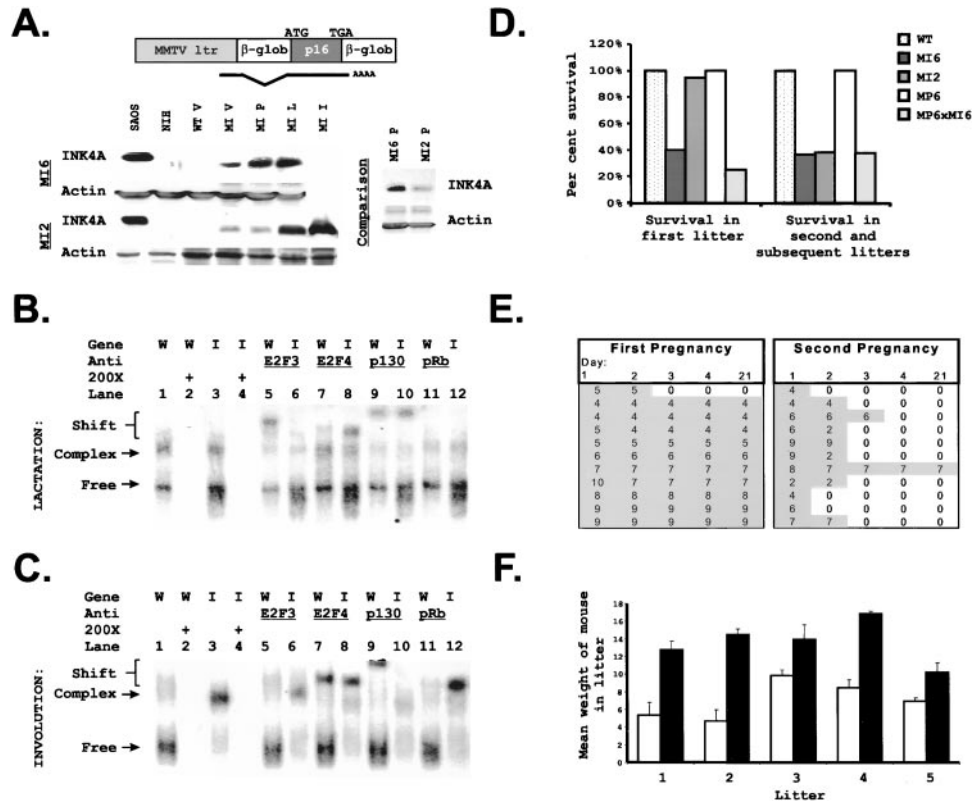


Fig. 2. Phenotypic changes in transgenic mice prematurely expressing p16 in mammary epithelium. *A*, a plasmid construct containing the MMTV enhancer and promoter region, a rabbit  $\beta$ -globin intron ( $\beta$ -glob), the human cDNA corresponding to the  $\alpha$ -transcript of INK4A (*p16*), and rabbit  $\beta$ -globin polyadenylation sequences ( $\beta$ -glob) was used to make transgenic mice. The highest expressing lines carrying the MMTV-p16 transgene (Tg.MI6 and MI2) were used for further analyses. Protein lysates from virgin, pregnant, lactating, and involuting mammary glands of wild-type (*WT*) and transgenic lines (Tg.MI6 and MI2, *Mi6* and *Mi2*) were compared using the JC1 monoclonal antibody, which only detects the transgenic human p16<sup>INK4A</sup> protein. Control lysates included SAOS2 cells (p16+), NIH3T3 cells (p16-), and wild-type virgin (*WT V*) mammary glands. The MI6 lactating sample is from day 2 of lactation when MI6 mice typically lost their litters. The MI2 lactation sample is from day 10, and the MI2 involution sample is from day 2. Pregnancy samples from day 10 in both transgenic strains were directly compared on the right side of this panel (*Comparison, MI6 P versus MI2 P*). p16 protein levels expressed during lactation in the MI2 strain were very similar to physiological p16 levels during involution. *B*, an EMSA compared E2F activity in MMTV-p16 (*MI2*) mammary glands during lactation (*Gene I*) with lactating wild-type (*Gene W*). Specificity was demonstrated by cold oligonucleotide competitions (*Lanes 2 and 4*). *Lanes 1 and 3* demonstrated no change in E2F/pocket protein complex activity in the p16 overexpressing mice. Supershifts were performed using the indicated antibodies (*Anti: E2F3, E2F4, p130, and pRb*). In this case, p16 expression increased E2F4 activity during lactation, as indicated by comparing the wild-type E2F3 supershifts (compare wild-type *Lanes 1, 5, and 7*) with the E2F4 supershifts in the MI2 mice (compare MI2 *Lanes 3, 6, and 8*). An antibody to p130 (*Anti, p130*) supershifted the complexed activity equally in the wild-type (*Lane 9*) and MI2 mice (*Lane 10*). No supershifts were seen using antibodies to pRb (*Anti: pRb, Lanes 11 and 12*). *C*, an EMSA compared E2F activity in MMTV-p16 (*MI2; Gene I*) mammary glands to wild-type mice (*Gene W*) on day two of involution. Specificity was demonstrated by cold oligonucleotide competitions (*Lanes 2 and 4*). *Lanes 1 and 3* demonstrated increased E2F/pocket protein complex activity in the p16-expressing mice identified by the increased intensity of the complexed band (*Complex*). Supershifts were performed using the indicated antibodies (*Anti E2F3, E2F4, p130, and pRb*). As before, the activity during wild-type involution was predominantly free E2F4 (compare wild-type *Lanes 1, 5, and 7*). In contrast, the activity in the MI2 mice was predominantly complexed E2F4 (compare *Lanes 3, 6, and 8*). Moreover, in this case the antibody to p130 (*Anti p130*) did not supershift the complexed activity in the MI2 mice (*Lane 10*), but supershifts were instead detected using an antibody to pRb (*Anti pRb, Lane 12*). *D*, litters born to MMTV-p16 transgenic mothers died in the first days of lactation. The percentage of litters surviving through lactation was compared between first and subsequent litters in the following genotypes: *WT*, wild type; *MI6*, Tg.MI6 prematurely expressing p16 during lactation; *MI2*, Tg.MI2 prematurely expressing lower levels of p16 during lactation; *MP6*, Tg.MP6 overexpressing cyclin D1; and *MP6xMI6*, doubly transgenic Tg.MP6/Tg.MI6 expressing both cyclin D1 and p16. Differences between wild-type and Tg.MI6 first litter survival were significant ( $P < 0.01$  by  $\chi^2$ ). The differences between the first and second litter survival rates of Tg.MI2 were significant ( $P < 0.05$  by  $\chi^2$ ). *E*, increased inhibitory effects of p16<sup>INK4A</sup> were seen after passage through mammary involution in a second p16<sup>INK4A</sup> transgenic line. We show numbers of offspring surviving on each of the indicated days after birth, comparing the outcome of first and second litters born to MI2 mothers. *F*, the mean weight of mice in surviving litters at weaning on day 21 born to Tg.MI2 mothers during their second pregnancy (*open columns*) was significantly decreased compared with litters born during their first pregnancy (*black columns*).

preparations confirmed the marked abnormalities in lobuloalveolar development in the MI6 strain (Fig. 3, compare *L* with *K*). These histological findings were consistent with the reported pattern of lobuloalveolar failure in cyclin D1 knockout mice (7) and suggested that mammary abnormalities in the cyclin D1 knockout mice could be completely explained by loss of cyclin-dependent kinase activity.

Litters born to the second p16<sup>INK4A</sup> transgenic strain (Tg.MI2) developed normally through a first pregnancy, lactation, and involution (Fig. 2*E*). The absence of lobuloalveolar defects during the first lactation in Tg.MI2 mice led us to speculate that p16<sup>INK4A</sup> expression levels must exceed a specific threshold before inhibiting lobuloalveolar growth (Fig. 2*A*). More importantly, this second strain also allowed us to evaluate the biochemical effects of an increase in the p16<sup>INK4A</sup> pulse during involution (Fig. 2*C*) and to assess the implications of this increase for subsequent pregnancies (Fig. 2*E*). Despite the augmented

p16<sup>INK4A</sup> in the Tg.MI2 strain, tissue regression proceeded normally after the first involution. We found no change in cellularity on day 7 of involution in Tg.MI2 mice, demonstrating that the additional p16 did not accelerate tissue regression (not shown). Instead, the appearance of a mammary phenotype in the second and subsequent pregnancies in this strain suggested that p16 might alter mammary growth potential in later mammary development (Fig. 3, *J* and *M*).

**Targeting of Cyclin D1 to Mammary Tissues during Involution Alters a Genetic Program of Terminal Differentiation without Affecting Net Cellular Proliferation.** We used MMTV-cyclin D1 transgenic mice (10) to evaluate the developmental importance of the normal loss of cyclin D1 expression during wild-type involution. A human-specific antibody identified human cyclin D1 corresponding to the transgene in Western blots (Fig. 4*A*). Transgenic cyclin D1 expression was seen at all stages in the cyclin D1 transgenic line and

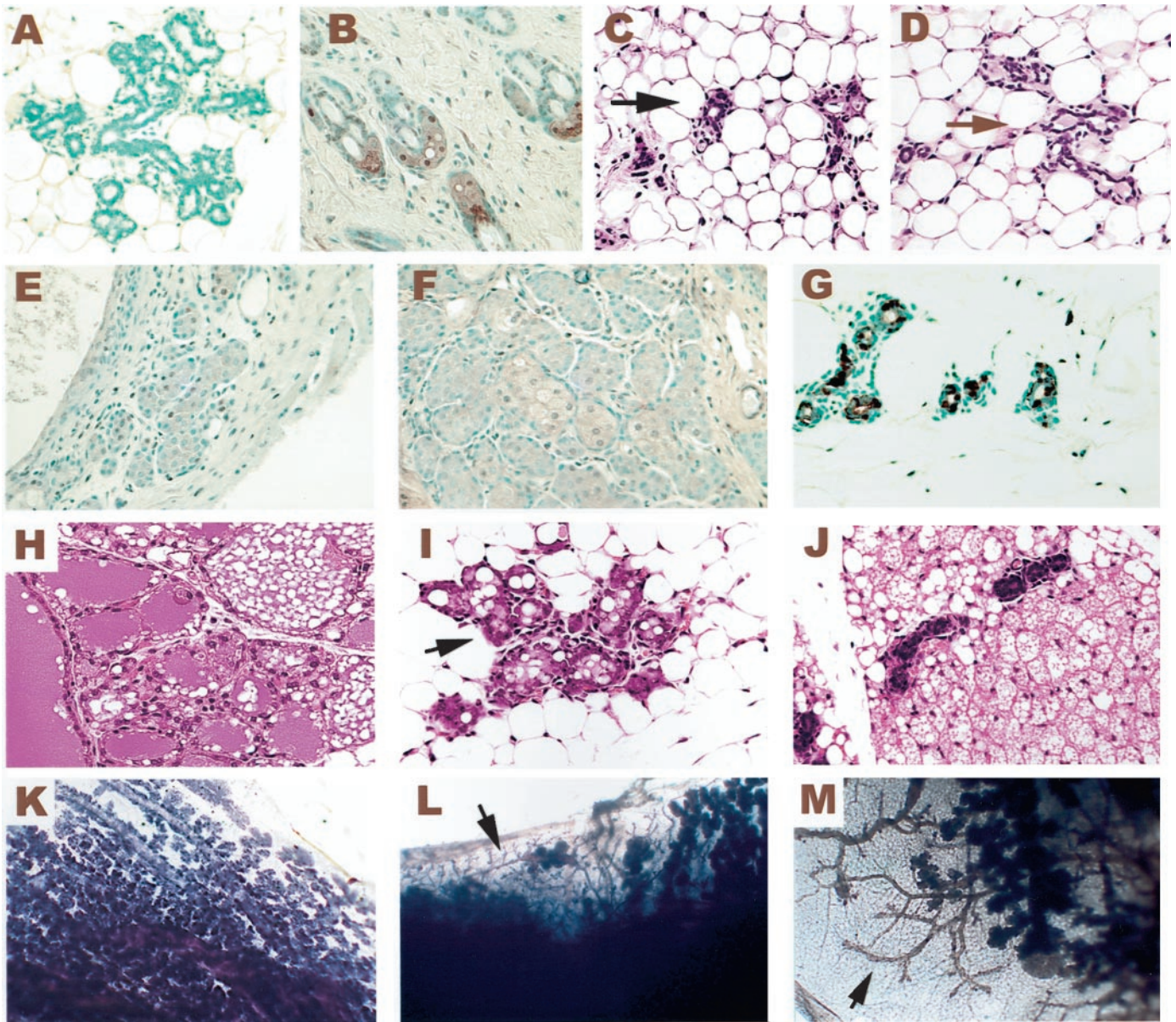


Fig. 3. A normal pulse of p16<sup>INK4A</sup> is sufficient but not necessary to arrest growth during normal mammary involution. *A* and *B*, a monoclonal antibody to murine p16<sup>INK4A</sup> identified mammary epithelial cells as the cell type expressing the novel pulse of p16 on day 2 of involution (*B*). Intense nuclear and cytoplasmic staining was detected in cells lining alveolar structures in regions approaching full regression in the wild-type mice. No staining was seen in pregnant mice (*A*). Involution samples processed using no primary antibody and a nonspecific primary antibody were also negative (not shown). p16 nullizygous mice (*D*) and wild-type mice (*C*) demonstrated identical cellularity of mammary epithelial tissues (arrows) in the two genotypes ( $\times 400$ ) on day 7 of involution. Histological sections from wild-type samples were immunostained on day 2 of involution using antibodies specific for murine p18 (*E*) and p19 (*F*). Negative controls for these studies included a pregnancy sample and samples processed with nonspecific primary antibodies (not shown). Nuclear p16 staining was also seen in the most poorly developed lobuloalveolar structures in MMTV-p16 transgenic mice (Tg.MI6) on day 2 of involution (*G*) when immunostained using a human-specific p16 monoclonal antibody. Negative controls for this study included a nonspecific primary antibody (not shown). Histological sections of wild-type and MMTV-p16<sup>INK4A</sup> mice were compared to evaluate phenotypic changes attributable to premature p16 expression. Photomicrographs ( $\times 400$ ) of wild-type and MMTV-p16 mice included lactating wild type (*H*) and lactating Tg.MI6 (*J*). Whole-mount preparations ( $\times 10$ ) included wild-type lactation (*K*) and Tg.MI6 lactation (*L*). Arrows, ductal structures lacking lobuloalveolar development. Photomicrographs and whole mounts from the second MMTV-p16<sup>INK4A</sup> line were compared to evaluate phenotypic changes attributable to a lower level of premature p16 expression. Shown are histological (*J*) and whole-mount appearances (*M*) of second lactation Tg.MI2 mice.

increased during involution in the transgenics. This prolongation of increased cyclin D1 expression during involution was also associated with loss of p16<sup>INK4A</sup> protein expression throughout involution, although neither p18 nor p19 levels were affected (Fig. 4A). This decrease in cyclin D1 expression during involution was not as marked in INK4A/ARF<sup>-/-</sup> null mice as in wild-type mice, although increased p18<sup>INK4C</sup> in the p16 null mice supported the view that p18 function may be redundant with p16 during mammary involution (Fig. 4A, additional bottom panels).

We next evaluated the role of cyclin D1 in regulation of E2F activity. We first demonstrated a 10-fold increase in free E2F activity

that was identified as E2F3 by supershift experiments during lactation (Fig. 4B, compare *Lanes 3* and *1* in the lactation panel, and *Lanes 5* and *6*). Cyclin D1 had even stronger effects during mammary involution at the time that mammary cells should stop dividing. We first found that E2F activity was predominantly in a complexed form during involution in the cyclin D1 transgenic mice and that cyclin D1 therefore abolished the appearance of a free E2F form (Fig. 4B, involution panels, compare *Lanes 3* and *1*). The complexed activity was predominantly E2F3 activity in the cyclin D1 mice (Fig. 4B, *Lanes 5–8*), and the complexes contained p130 (*Lane 10*). Thus, cyclin D1 overexpression induced additional E2F3 during both lacta-



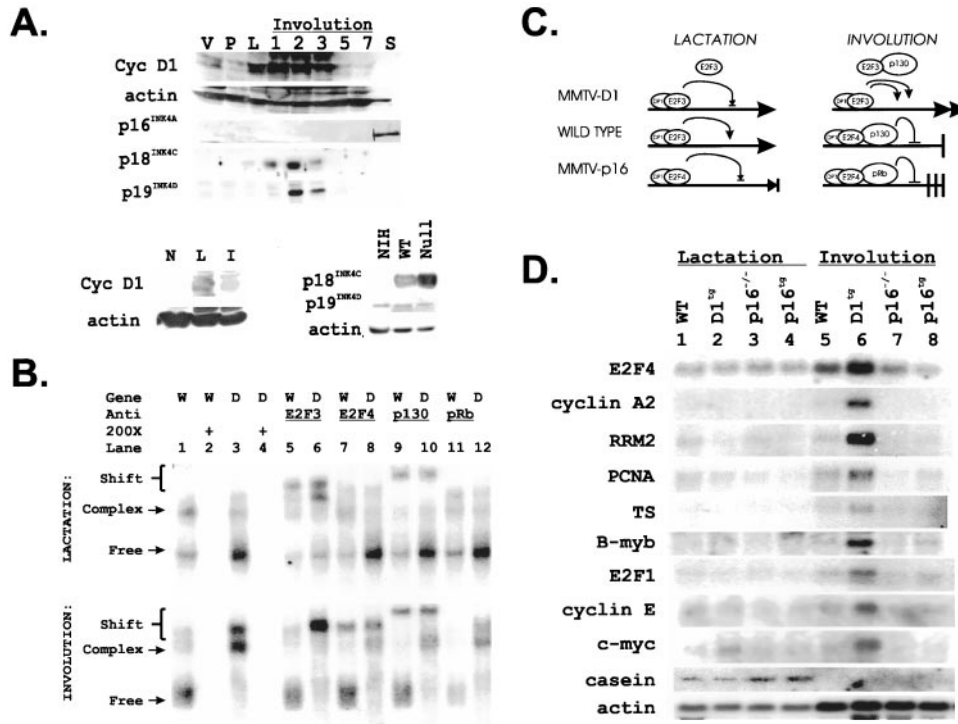


Fig. 4. Cyclin D1 expression alters patterns of E2F binding activity associated with growth arrest and terminal differentiation. *A*, expression of cyclin D1 in mammary glands from MMTV-cyclin D1 transgenic mice (Tg.MP6) was detected with a monoclonal antibody that detects transgenic human cyclin D1 (*Cyc D1*). The negative control contains lysates from SAOS2 cells (*S*). Simultaneously probed lysates from MMTV-cyclin D1 mice using the anti-INK4A antibody (JC2) revealed a positive signal in the SAOS2 (*S*) control, but INK4A was absent from all other samples. These lysates still expressed p18<sup>INK4C</sup> and p19<sup>INK4D</sup> (bottom two panels, *INK4C* and *INK4D*). An actin loading control is shown. The bottom left panel demonstrates cyclin D1 expression in p16 null mice during lactation (*L*) and involution (*I*). The bottom right panel compares p18<sup>INK4C</sup> and p19<sup>INK4D</sup> levels during involution between wild-type (*WT*) and p16 null (*Null*) mice. An actin loading control is shown. Negative expression controls include NIH3T3 cells (*NIH*) and mammary extracts from lactating cyclin D1 *-/-* (*N*) mice. *B*, EMSAs compared E2F activities in lactation and involution in MMTV-cyclin D1 transgenic mice. Cold competitors are included as indicated ( $\times 200$ ), Lanes 2 and 4). During lactation, a 10-fold increase in free E2F activity was identified as E2F3 by supershifts (compare Lanes 6 and 3 to Lanes 5 and 1). During involution, the transition to E2F4 activity in the wild-type mice (comparing Lanes 1 and 7 for the E2F4 supershift) was not observed in the MMTV-cyclin D1 mice. Instead, the E2F activity in MMTV-cyclin D1 mice appeared in the slower migrating complexed form (compare Lanes 3 and 1). In addition, E2F activity during involution was only supershifted by antibodies to E2F3 in the MMTV cyclin D1 mice (compare Lanes 3 and 6). *C*, we observed E2F activities that match predictions of the active repressor model of E2F function. Mice of the three genotypes including MMTV-cyclin D1 (*MMTV-D1*), wild-type (*Wild Type*), and *MMTV-p16* in *Lactation* and *Involution* are compared. An active repressor complex containing E2F4, DP1, and p130 is found during normal mammary involution. Cyclin D1 expression during normal lactation increased free E2F3. E2F3 appears to titrate E2F4 out of its repressor form during involution in the MMTV-cyclin D1 strain. In contrast, p16 promotes the formation of E2F4-DP1 repressor complexes and promotes assembly with pRb during involution in the MMTV-p16 strain. *D*, we tested mRNA expression patterns for 20 E2F target genes (46). We compared wild-type (*WT*), MMTV-cyclin D1 (*D1<sup>tg</sup>*), p16 nullizygous (*INK4A/ARF<sup>-/-</sup>*), and MMTV-p16 transgenic mice (*p16<sup>tg</sup>*) on lactation day 10 and involution day 2 (indicated). Overexpression of cyclin D1 increased expression of E2F4, cyclin A2, ribonucleotide reductase (*RRM2*), thymidylate synthetase (*TS*), *B-myb*, E2F1, cyclin E, and *c-myc*. Casein mRNA expression during lactation did not vary among the genotypes. An actin loading control is shown.

tion and involution. This E2F3 remained in the free form in lactating cyclin D1 mice.

Taken together, our data provide important *in vivo* evidence that cyclin D1 acts to derepress an active repressor form of E2F (Fig. 4C). The E2F proteins regulate a variety of well-characterized genes needed for progression through S-phase. The response of these E2F target genes to transgenic cyclin D1 expression should differentiate between its potential function as an activator of E2F targets that promote G<sub>1</sub>-S progression during lactation or as a derepressor of E2F target genes during involution. We therefore evaluated the response of a standard set of E2F target genes (36) to perturbations of cyclin D1 and p16 expression during lactation and involution (Fig. 4D). Prolongation of cyclin D1 expression into involution caused a striking and consistent pattern of alterations in E2F target gene regulation that was not seen in either the *INK4A/ARF<sup>-/-</sup>* or *MMTV-p16* mice. None of the three genetic alterations had marked effects on E2F target gene activity during lactation (Fig. 4D, first four lanes of each panel), although cyclin D1 overexpression slightly increased *c-myc* levels. In contrast, the expression level of each E2F target gene examined was markedly increased during involution in the MMTV-cyclin D1 transgenics. Furthermore, neither loss nor gain of p16 affected any of the same set of target genes at that time. We also found no change in

casein levels during lactation, demonstrating no change in differentiated function in any of the strains.

The absence of E2F target gene regulation in mice that have either lost or gained p16 during involution contrasts with the effects of cyclin D1 and suggests that cyclin D1 and p16 regulate somewhat different functions during involution. We confirmed this possibility by mating MMTV-cyclin D1 mice to MMTV-p16 mice, where we found that overexpression of cyclin D1 did not repair the lactational phenotype in the MI6 strain (Fig. 2D).

Increased cellular growth rates, delayed growth arrest, or decreased tissue regression should increase epithelial cellularity at the end of mammary involution, if cyclin D1 is primarily regulating those processes in mammary development. Surprisingly, at the end of a single pregnancy cycle, we found no difference in epithelial cellularity between wild-type and MMTV-cyclin D1 mice when involution was completed (Fig. 5, A and B). In these photomicrographs, mammary tissue appears as islands of epithelial cells in a background of stromal tissue. The numbers of epithelial islands and the number of cells in individual islands were equivalent in cyclin D1-expressing and normal tissues.

The histological appearance of MMTV-cyclin D1 mammary glands could not be distinguished from wild-type mice for several months

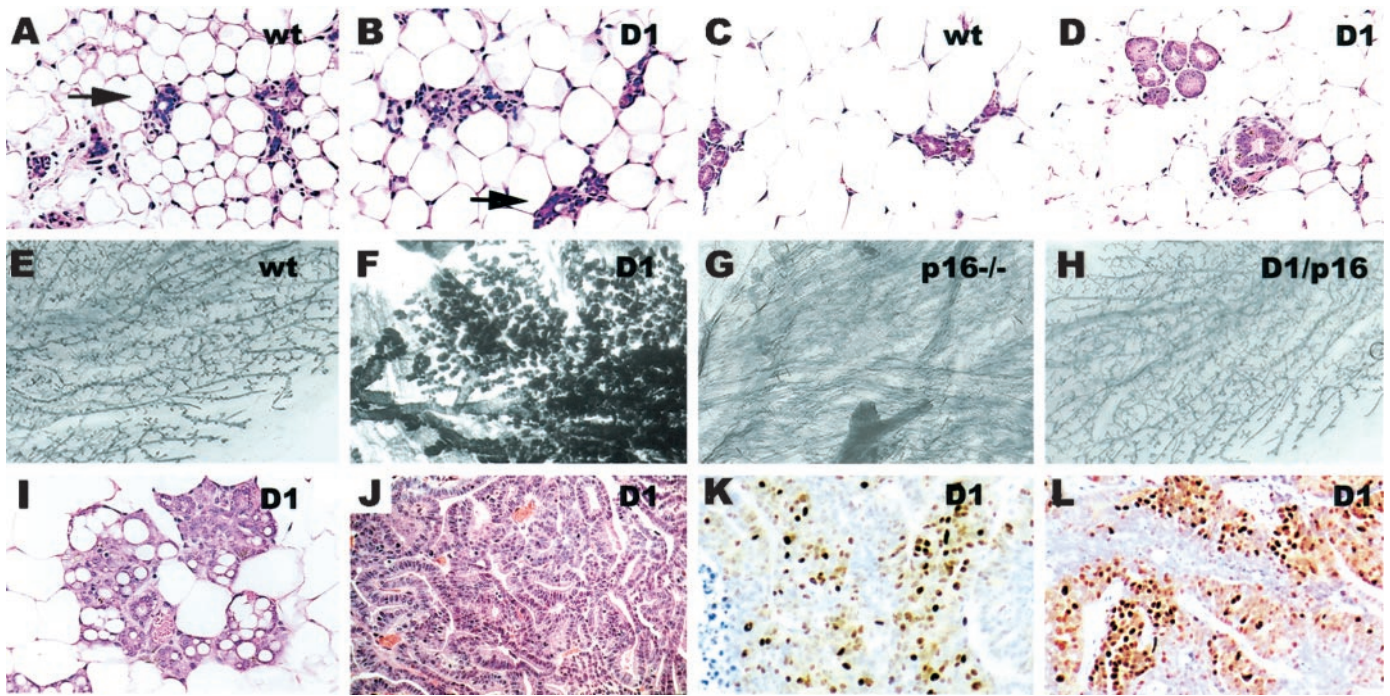


Fig. 5. Stable hyperplastic changes developed in mammary glands expressing cyclin D1 late after normal histology is seen at the completion of involution. Photomicrographs of histological sections of wild-type and MMTV-cyclin D1 mice. On the seventh day after weaning, epithelial islands (arrows) comprising equivalent portions of the mammary gland demonstrated identical cellularity in wild-type (A) and MMTV-cyclin D1 transgenics (B;  $\times 400$ ). Four months after completion of pregnancy in the cyclin D1 transgenic mice, renewed proliferation of the lobuloalveolar cells became histologically evident as focal proliferation of islands of mammary epithelium comparing wild-type (C) and transgenic mice (D). Photomicrographs of whole-mount preparations ( $\times 10$ ) of mammary glands demonstrated the proliferative status of the mouse mammary tree 4 months after weaning in the three genotypes studied (E–H). Shown are whole-mount preparations from a wild-type mouse (E) and a cyclin D1 transgenic mouse 4 months after a single pregnancy (F). The renewed focal lobuloalveolar development was not evident in p16 nullizygous (G) or doubly transgenic MMTV-cyclin D1/MMTV-p16 transgenic mice (H). Lobuloalveolar proliferation progressed, and dysplasia was observed by 12 months of age (I) in the MMTV-cyclin D1 mice ( $\times 400$ ). Adenocarcinomas (J) appeared by  $\sim 18$  months of age. The MMTV-cyclin D1-induced tumors expressed the human cyclin D1 as demonstrated by immunohistochemical staining (K and L;  $\times 400$ ).

after completion of a single pregnancy. Evidence for subsequent focal nodular growth of lobuloalveolar epithelium first appeared 4 months later when focal hyperplastic nodules were demonstrated in whole-mount preparations of the MMTV-cyclin D1 transgenic mice (Fig. 5, compare F with E). These renewed hyperplastic changes (Fig. 5, D versus C) occurred in mice that had completed a single pregnancy and were not pregnant at the time of harvest. These changes have not been observed in older nulliparous MMTV-cyclin D1 mice (not shown). In contrast to the initial diffuse hyperplastic changes in pregnant cyclin D1 transgenic mice (10), these delayed lesions were focal, stable, and exhibited progressive acquisition of atypical cellular characteristics (Fig. 5J). We also examined whole-mount preparations of MMTV-cyclin D1/MMTV-p16 transgenic mice and INK4A/ARF $^{-/-}$  mice (Fig. 5, G and H) and found that loss of p16 alone was not sufficient to account for the changes seen in the MMTV-cyclin D1 mice. Finally, these initial hyperplastic and dysplastic changes were followed by adenocarcinomas 6–8 months later in the cyclin D1 transgenic mice (Fig. 5J), which expressed the human cyclin D1 at high levels (Fig. 5, K and L).

To determine whether cyclin D1 expanded a population of potential stem cells, we analyzed clonality of tumors arising in the MMTV-cyclin D1 transgenic mice. Although retroviral infections are usually used to identify collaborating oncogenes in transgenic experiments, they also provide a measure of clonality in tumors. We initially sought to identify oncogenes collaborating with cyclin D1 in mammary tumorigenesis by infecting wild-type mice and MMTV-cyclin D1 transgenic mice with a cloned strain of MMTV. Importantly, MMTV infection of the cyclin D1 transgenics did not accelerate tumorigenesis when compared with the infected wild-type mice (Fig. 6A). Tumor onset was the same as we observed previously in uninfected MMTV-

cyclin D1 transgenics,  $505 \pm 113$  days compared with  $534 \pm 35$  days (10). Despite finding no evidence of collaboration between cyclin D1 and MMTV insertions, we did find that the tumors in the MMTV-cyclin D1 transgenic were derived from multiple independent infection events (Fig. 6B). Thus, tumor masses appeared at the same rate in the MMTV-infected wild-type and MMTV-infected cyclin D1 mice but arose from an expanded population of infectable target cells in the MMTV-cyclin D1 transgenic mice.

## DISCUSSION

Although perturbations in cyclin D1/Cdk4, p16, or pRb are central to tumorigenesis (17), their cell cycle functions are not essential for completion of most normal cell division cycles (6, 7, 35, 37). This paradox is emphasized by the general inability of G<sub>1</sub> cyclins to increase net proliferation in cells despite accelerating G<sub>1</sub> to S progression (20). In contrast, the potential contributions of cell cycle regulators to terminal differentiation have obvious implications for tumorigenesis (21–23). Despite the potential importance of their role in terminal differentiation, surprisingly little is known about this function *in vivo*.

We found a novel pulse of p16 expression during normal mammary involution that has not been observed previously in other tissues. The contribution of p16 to normal growth arrest in a mature tissue is particularly interesting because a physiological role for this specific antagonist of cyclin D signaling has not yet been identified (38). This physiological p16 pulse directly regulated E2F4/pocket protein complex formation, and it directly contributed to growth arrest. However, growth arrest progressed normally in the INK4A/ARF $^{-/-}$  strain, indicating that this pulse is not required for growth arrest. Although



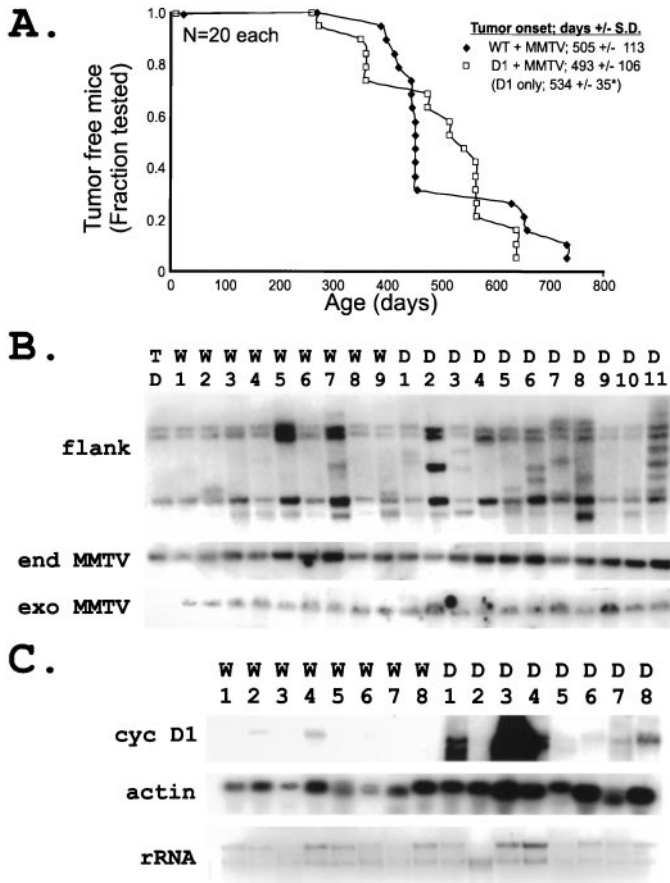


Fig. 6. MMTV infection demonstrates increased clonality in MMTV-cyclin D1 transgenic mice. *A*, time to discovery of palpable tumors is plotted for mice infected with a cloned MMTV isolate. Tumor-free survival of MMTV-infected wild-type mice (*WT*) is compared with MMTV-infected MMTV-cyclin D1 mice and uninfected MMTV-cyclin D1 mice (14). *B*, clonality of tumors was tested by Southern hybridizations. 3' sequences flanking the insertion sites (*flank*) of integrated MMTV in the wild-type (*W*) and MMTV-cyclin D1 transgenic mice (*D*) were first identified with an *env* probe in *HindIII* cut DNA. Tail DNA (*T*) from an uninfected MMTV-cyclin D1 transgenic mouse is included to identify endogenous MMTV. Endogenous (*end MMTV*) proviral sequences were identified in *BglIII* cut samples to control for variations in DNA loading. Successful infection with the pathogenic hybrid MMTV (*exo MMTV*) was demonstrated by the presence of exogenous *env* sequences. *C*, RNA blots from the indicated tumors from wild type (*W*) and MMTV-cyclin D1 transgenic mice (*D*) were probed for cyclin D1 (*cyc D1*) and actin. The ethidium bromide-stained gel (*rRNA*) is shown.

p18<sup>INK4C</sup> and p19<sup>INK4D</sup> have been phenomenologically associated with embryonic neural differentiation (39), neither contributed directly to this process *in vivo* (40). Although p21<sup>CIP</sup> functions in myoblast differentiation *in vitro* (41), it is far less significant *in vivo* (42). Thus, our study provides novel *in vivo* evidence that a specific Cdk4/6 inhibitor directly contributes to growth arrest.

The E2F activities we observed in the various developmental stages of pregnancy provide an important *in vivo* confirmation of the active repressor model of E2F function (Fig. 4C; Ref. 43). During pregnancy and lactation, free E2F3 predominated in wild-type mice (Fig. 1E). During wild-type involution, decreased cyclin D1 together with increased p16 were associated with assembly of an E2F4-p130 repressor complex (Fig. 1, E and F). Cyclin D1 overexpression had two effects in the MMTV-cyclin D1 mice (Fig. 4): (a) it promoted additional free E2F3 activity during lactation; and (b) the association of p130 with E2F3 during involution in cyclin D1 transgenics titrated p130 away from the E2F4-p130 repressor complex, thereby derepressing all E2F target genes simultaneously. In contrast, expression of p16 promoted a switch to E2F4 activity during lactation (Fig. 2). The additional p16 present during involution in this transgenic strain was then sufficient

to promote additional E2F4-pocket protein assembly with pRb. Interestingly, the most significant effect of all of these regulatory changes was simultaneous derepression of all E2F target genes only during involution in the cyclin D1 transgenics.

Why are two interdependent signaling molecules regulated during mammary involution? The phenotype of the two MMTV-p16 transgenic lines clearly implicates p16 as a regulator of growth arrest. However, the phenotype of the MMTV-cyclin D1 mice identifies a far more complex issue, suggesting that cyclin D1 actually regulates the proliferative potential of the mammary gland after passage through pregnancy and involution. Consistent with every other test using cyclin D overexpression, increased cyclin D1 did not promote additional cell divisions in the cyclin D1 mice. Instead, it derepressed a critical set of E2F target genes during a transition to a terminally differentiated state.

At least four models are consistent with our findings: (a) the delayed development of focal nodular hyperplasia suggests that these hyperplastic nodules might expand from an expanded population of stem cells that failed to undergo normal terminal differentiation; (b) alternatively, the focal proliferations might represent stochastic escape from global repression of the G<sub>1</sub>-S regulatory machinery; (c) the loss of normal growth arrest during involution in the cyclin D1 mice may abrogate a “checkpoint” elimination of mammary epithelial cells that have accumulated genetic mutations during the growth cycle of pregnancy; and (d) target cells for cyclin D1 in transformation might be expanded during pregnancy and lactation, independent of cyclin D1 effects during these periods. In this scenario, the critical “execution” period for the effects of cyclin D1 may not be until after involution when the cells would normally be quiescent.

The MMTV result is particularly provocative. In the first two models, we would expect to find expanded targets for MMTV infections, because both mechanisms increase the dividing cell populations that are needed to support retroviral integration. However, our infected cyclin D1 transgenics did not exhibit accelerated tumorigenesis, despite the presence of new exogenous proviruses. Although this might result from an inefficient infection of the mice, the presence of multiple new exogenous proviruses in the majority of tumors argues against it. Furthermore, MMTV infection accelerates tumorigenesis in several other transgenic mouse models (44–46). More likely, this result reflects the intimate involvement of cyclin D1 in the pathways of most or all of the targets for MMTV insertion mutations including both Wnts and Fgfs (47, 48).

Delayed menarche, pregnancy at a young age, multiple pregnancies, multiparity, breast feeding, and early menopause all decrease the incidence of breast cancer in humans (1, 49). Many mechanisms for this protective effect have been proposed (50). Mechanistic studies in rodents identified enhanced terminal differentiation as one key result of pregnancy (4, 51). The pattern of litter loss in the MI2 strain of MMTV-p16 mice provides a potential confirmation of this effect. Loss of litters in the second and subsequent pregnancies confirms that the proliferative capacity of the mammary glands decreases after passage through pregnancy.

We identified normal and critical functions for regulated changes of both cyclin D1 and p16 levels during mammary involution. Although cyclin D1 is known to regulate G<sub>1</sub>-S progression, its functions in differentiation are poorly understood. Although the significance of p16<sup>INK4A</sup> loss in tumorigenesis has been repeatedly shown in numerous studies, little is known about its normal functions. Importantly, the ability to regulate growth arrest in the involuting mammary gland is one p16<sup>INK4A</sup> function that is clearly independent of p19<sup>INK4AβARF</sup> (28). Future studies of both cyclin D1 and p16<sup>INK4A</sup> regulation and function during mammary involution may clarify the nature of the



protective effect of pregnancy, which has otherwise been approachable only as an epidemiological risk factor in human breast cancers.

## ACKNOWLEDGMENTS

We sadly report that our friend, colleague, and co-author, Dr. Zeljko Nikolic, died of a recurrent Ewing's sarcoma on August 27, 2001 while we were revising the manuscript. He was training in the Massachusetts General Hospital Pediatric Residency program at the time of his death. His loss is doubly tragic because it occurred 12 years after his initially successful treatment and because his contributions to pediatric oncology would have been profound.

We thank Drs. Dan Haber, Dennis Sgroi, John Branda, and Nick Dyson for helpful discussions. We thank Dr. Sander van den Heuvel for critical reading of the manuscript. We thank Michael Previte, Kelly Johnston, and Dr. Yuhua Nong for expert technical assistance. Murine INK4A-D plasmids and antibodies were generously provided by Drs. Chuck Sherr, St. Jude Children's Research Hospital, Memphis, TN, and Dawn Quelle, University of Iowa, Iowa City, IA. The *p16* locus knockout strain was the generous gift of Drs. Ned Sharpless and Ron DePinho of the Dana-Farber Cancer Institute, Boston, MA.

## REFERENCES

- Harris, J. R., Lippman, M. E., Veronesi, U., and Willett, W. Breast cancer. *N. Engl. J. Med.*, **327**: 319–328, 1992.
- Lipworth, L., Bailey, L. R., and Trichopoulos, D. History of breast-feeding in relation to breast cancer risk: a review of the epidemiologic literature. *J. Natl. Cancer Inst.*, **92**: 302–312, 2000.
- Chie, W. C., Hsieh, C., Newcomb, P. A., Longnecker, M. P., Mittendorf, R., Greenberg, E. R., Clapp, R. W., Burke, K. P., Titus-Ernstoff, L., Trentham-Dietz, A., and MacMahon, B. Age at any full-term pregnancy and breast cancer risk. *Am. J. Epidemiol.*, **151**: 715–722, 2000.
- Russo, I. H., and Russo, J. Mammary gland neoplasia in long-term rodent studies. *Environ. Health Perspect.*, **104**: 938–967, 1996.
- Russo, J., Wilgus, G., and Russo, I. H. Susceptibility of the mammary gland to carcinogenesis. I. Differentiation of the mammary gland as determinant of tumor incidence and type of lesion. *Am. J. Pathol.*, **96**: 721–736, 1979.
- Fantl, V., Stamp, G., Andrews, A., Rosewell, I., and Dickson, C. Mice lacking cyclin D1 are small and show defects in eye and mammary gland development. *Genes Dev.*, **9**: 2364–2372, 1995.
- Sicinski, P., Donaher, J. L., Parker, S. B., Li, T., Fazeli, A., Gardner, H., Haslam, S. Z., Bronson, R. T., Elledge, S. J., and Weinberg, R. A. Cyclin D1 provides a link between development and oncogenesis in the retina and breast. *Cell*, **82**: 621–630, 1995.
- Peters, G., Fantl, V., Smith, R., Brookes, S., and Dickson, C. Chromosome 11q13 markers and D-type cyclins in breast cancer. *Breast Cancer Res. Treat.*, **33**: 125–135, 1995.
- Zuckerberg, L. R., Yang, W. I., Gadd, M., Thor, A. D., Koerner, F. C., Schmidt, E. V., and Arnold, A. Cyclin D1 (PRAD1) protein expression in breast cancer: approximately one-third of infiltrating mammary carcinomas show overexpression of the *cyclin D1* oncogene. *Mod. Pathol.*, **8**: 560–567, 1995.
- Wang, T. C., Cardiff, R. D., Zuckerberg, L., Lees, E., Arnold, A., and Schmidt, E. V. Mammary hyperplasia and carcinoma in MMTV-cyclin D1 transgenic mice. *Nature (Lond.)*, **369**: 669–671, 1994.
- Bodrug, S. E., Warner, B. J., Bath, M. L., Lindeman, G. J., Harris, A. W., and Adams, J. M. Cyclin D1 transgene impedes lymphocyte maturation and collaborates in lymphomagenesis with the *myc* gene. *EMBO J.*, **13**: 2124–2130, 1994.
- Nakagawa, H., Wang, T. C., Zuckerberg, L., Odze, R., Togawa, K., May, G. H., Wilson, J., and Rustgi, A. K. The targeting of the *cyclin D1* oncogene by an Epstein-Barr virus promoter in transgenic mice causes dysplasia in the tongue, esophagus and forestomach. *Oncogene*, **14**: 1185–1190, 1997.
- Robles, A. I., Larcher, F., Whalin, R. B., Murillas, R., Richie, E., Gimenez-Conti, I. B., Jorcano, J. L., and Conti, C. J. Expression of cyclin D1 in epithelial tissues of transgenic mice results in epidermal hyperproliferation and severe thymic hyperplasia. *Proc. Natl. Acad. Sci. USA*, **93**: 7634–7638, 1996.
- Chellappan, S. P., Hiebert, S., Mudryj, M., Horowitz, J. M., and Nevins, J. R. The E2F transcription factor is a cellular target for the RB protein. *Cell*, **65**: 1053–1061, 1991.
- Weintraub, S. J., Prater, C. A., and Dean, D. C. Retinoblastoma protein switches the E2F site from positive to negative element. *Nature (Lond.)*, **358**: 259–261, 1992.
- Sherr, C. J., and Roberts, J. M. Inhibitors of mammalian G1 cyclin-dependent kinases. *Genes Dev.*, **9**: 1149–1163, 1995.
- Sherr, C. J. Cancer cell cycles. *Science (Wash. DC)*, **274**: 1672–1677, 1996.
- Huschtscha, L. I., Noble, J. R., Neumann, A. A., Moy, E. L., Barry, P., Melki, J. R., Clark, S. J., and Reddel, R. R. Loss of p16INK4 expression by methylation is associated with lifespan extension of human mammary epithelial cells. *Cancer Res.*, **58**: 3508–3512, 1998.
- Tshilias, J., Kapusta, L., and Slingerland, J. The prognostic significance of altered cyclin-dependent kinase inhibitors in human cancer. *Annu. Rev. Med.*, **50**: 401–423, 1999.
- Quelle, D. E., Ashmun, R. A., Shurtleff, S. A., Kato, J. Y., Bar-Sagi, D., Roussel, M. F., and Sherr, C. J. Overexpression of mouse D-type cyclins accelerates G1 phase in rodent fibroblasts. *Genes Dev.*, **7**: 1559–1571, 1993.
- Di Cunto, F., Topley, G., Calautti, E., Hsiao, J., Ong, L., Seth, P. K., and Dotto, G. P. Inhibitory function of p21Cip1/WAF1 in differentiation of primary mouse keratinocytes independent of cell cycle control. *Science (Wash. DC)*, **280**: 1069–1072, 1998.
- Parker, S. B., Eichele, G., Zhang, P., Rawls, A., Sands, A. T., Bradley, A., Olson, E. N., Harper, J. W., and Elledge, S. J. p53-independent expression of p21cip1 in muscle and other terminally differentiating cells. *Science (Wash. DC)*, **267**: 1024–1027, 1995.
- Hamel, P. A., Phillips, R. A., Muncaster, M., and Gallie, B. L. Speculations on the roles of RB1 in tissue-specific differentiation, tumor initiation, and tumor progression. *FASEB J.*, **7**: 846–854, 1993.
- Motokura, T., Bloom, T., Kim, H. G., Juppner, H., Ruderman, J. V., Kronenberg, H. M., and Arnold, A. A novel cyclin encoded by a *bell*-linked candidate oncogene. *Nature (Lond.)*, **350**: 512–515, 1991.
- Koh, J., Enders, G. H., Dynlacht, B. D., and Harlow, E. Tumour-derived *p16* alleles encoding proteins defective in cell-cycle inhibition. *Nature (Lond.)*, **375**: 506–510, 1995.
- Matsumine, H., Roussel, M. F., Ashmun, R. A., and Sherr, C. J. Colony-stimulating factor 1 regulates novel cyclins during the G1 phase of the cell cycle. *Cell*, **65**: 701–713, 1991.
- Quelle, D. E., Ashmun, R. A., Hannon, G. J., Rehberger, P. A., Trono, D., Richter, K. H., Walker, C., Beach, D., Sherr, C. J., and Serrano, M. Cloning and characterization of murine *p16INK4a* and *p15INK4b* genes. *Oncogene*, **11**: 635–645, 1995.
- Quelle, D. E., Zindy, F., Ashmun, R. A., and Sherr, C. J. Alternative reading frames of the *INK4a* tumor suppressor gene encode two unrelated proteins capable of inducing cell cycle arrest. *Cell*, **83**: 993–1000, 1995.
- Huang, A. L., Ostrowski, M. C., Berard, D., and Hager, G. L. Glucocorticoid regulation of the Ha-MuSV *p21* gene conferred by sequences from mouse mammary tumor virus. *Cell*, **27**: 245–255, 1981.
- Strange, R., Li, F., Saurer, S., Burkhardt, A., and Friis, R. R. Apoptotic cell death and tissue remodelling during mouse mammary gland involution. *Development (Camb.)*, **115**: 49–58, 1992.
- Shackleford, G. M., and Varmus, H. E. Construction of a clonable, infectious, and tumorigenic mouse mammary tumor virus provirus and a derivative genetic vector. *Proc. Natl. Acad. Sci. USA*, **85**: 9655–9659, 1988.
- Harlow, E., and Lane, D. *Antibodies: A Laboratory Manual*. Cold Spring Harbor, NY: Cold Spring Harbor Laboratory, 1988.
- Hirai, H., Roussel, M. F., Kato, J. Y., Ashmun, R. A., and Sherr, C. J. Novel INK4 proteins, p19 and p18, are specific inhibitors of the cyclin D-dependent kinases CDK4 and CDK6. *Mol. Cell. Biol.*, **15**: 2672–2681, 1995.
- Russo, J., Gusterson, B. A., Rogers, A. E., Russo, I. H., Wellings, S. R., and van Zwieten, M. J. Comparative study of human and rat mammary tumorigenesis. *Lab. Invest.*, **62**: 244–278, 1990.
- Serrano, M., Lee, H., Chin, L., Cordon-Cardo, C., Beach, D., and DePinho, R. A. Role of the *INK4a* locus in tumor suppression and cell mortality. *Cell*, **85**: 27–37, 1996.
- Hurford, R. K., Jr., Cobrinik, D., Lee, M. H., and Dyson, N. pRB and p107/p130 are required for the regulated expression of different sets of E2F responsive genes. *Genes Dev.*, **11**: 1447–1463, 1997.
- Jacks, T., Fazeli, A., Schmitt, E. M., Bronson, R. T., Goodell, M. A., and Weinberg, R. A. Effects of an Rb mutation in the mouse. *Nature (Lond.)*, **359**: 295–300, 1992.
- Sherr, C. J., and Roberts, J. M. CDK inhibitors: positive and negative regulators of G1-phase progression. *Genes Dev.*, **13**: 1501–1512, 1999.
- Zindy, F., Soares, H., Herzog, K. H., Morgan, J., Sherr, C. J., and Roussel, M. F. Expression of INK4 inhibitors of cyclin D-dependent kinases during mouse brain development. *Cell Growth Differ.*, **8**: 1139–1150, 1997.
- Zindy, F., van Deursen, J., Grosveld, G., Sherr, C. J., and Roussel, M. F. INK4-deficient mice are fertile despite testicular atrophy. *Mol. Cell. Biol.*, **20**: 372–378, 2000.
- Skapek, S. X., Rhee, J., Spicer, D. B., and Lassar, A. B. Inhibition of myogenic differentiation in proliferating myoblasts by cyclin D1-dependent kinase. *Science (Wash. DC)*, **267**: 1022–1024, 1995.
- Zhang, P., Wong, C., De Pinho, R., Harper, J. W., and Elledge, S. J. Cooperation between the Cdk inhibitors p27 KIP1 and p57 KIP2 in the control of tissue growth and development. *Genes Dev.*, **12**: 3162–3167, 1998.
- Dyson, N. The regulation of E2F by pRB-family proteins. *Genes Dev.*, **12**: 2245–2262, 1998.
- Schroeder, J. A., Troyer, K. L., and Lee, D. C. Cooperative induction of mammary tumorigenesis by TGF $\alpha$  and Wnts. *Oncogene*, **19**: 3193–3199, 2000.
- Lee, F. S., Lane, T. F., Kuo, A., Shackleford, G. M., and Leder, P. Insertional mutagenesis identifies a member of the *Wnt* gene family as a candidate oncogene in the mammary epithelium of int-2/Fgf-3 transgenic mice. *Proc. Natl. Acad. Sci. USA*, **92**: 2268–2272, 1995.
- Shackleford, G. M., MacArthur, C. A., Kwan, H. C., and Varmus, H. E. Mouse mammary tumor virus infection accelerates mammary carcinogenesis in Wnt-1 transgenic mice by insertional activation of int-2/Fgf-3 and hst/Fgf-4. *Proc. Natl. Acad. Sci. USA*, **90**: 740–744, 1993.
- Boudreau, N., Andrews, C., Srebrow, A., Ravanpay, A., and Cheresch, D. A. Induction of the angiogenic phenotype by Hox D3. *J. Cell Biol.*, **139**: 257–264, 1997.
- Rimerman, R. A., Gellert-Randleman, A., and Diehl, J. A. Wnt1 and MEK1 cooperate to promote cyclin D1 accumulation and cellular transformation. *J. Biol. Chem.*, **275**: 14736–14742, 2000.
- Kelsey, J. L., Gammon, M. D., and John, E. M. Reproductive factors and breast cancer. *Epidemiol. Rev.*, **15**: 36–47, 1993.
- Pike, M. C., Spicer, D. V., Dahmouh, L., and Press, M. F. Estrogens, progestogens, normal breast cell proliferation, and breast cancer risk. *Epidemiol. Rev.*, **15**: 17–35, 1993.
- Russo, I. H., and Russo, J. Role of hormones in mammary cancer initiation and progression. *J. Mammary Gland Biol. Neoplasia*, **3**: 49–61, 1998.